Effects of shoe longitudinal bending stiffness and runner level on Achilles tendon loading in experienced and novice male runners: a musculoskeletal modelling study

Shixin Lin
Ningbo University
Hao Yuan
Wenzhou University
Jiaying Shao
Ningbo University
Dongwei Liu
Zhejiang University of Finance and Economics
Mianfang Ruan
Wenzhou University
Ye Ma
maye@nbu.edu.cn

Ningbo University

Article

Keywords: Achilles tendon force, longitudinal bending stiffness, musculoskeletal modeling, running biomechanics, experienced runner

Posted Date: July 13th, 2026

DOI: https://doi.org/10.21203/rs.3.rs-9811102/v1

Additional Declarations: No competing interests reported.

Effects of shoe longitudinal bending stiffness and runner level on Achilles tendon loading in experienced and novice male runners: a musculoskeletal modelling study

Shixin Lin[1#], Hao Yuan[2#], Jiaying Shao[1], Dongwei Liu[3], Mianfang Ruan[2*], Ye Ma[1*]

[1] Research Academy of Grand Health, Faculty of Sports Sciences, Ningbo University, Ningbo 315211, China

[2] College of Physical Education and Health, Wenzhou University, Wenzhou 325000, China

[3] School of Information Technology and Artificial Intelligence, Zhejiang University of Finance and Economics, Hangzhou 310018, China

[#] The authors contribute equally.

Corresponding Authors: Mianfang Ruan, mianfangruan@wzu.edu.cn; Ye Ma, maye@nbu.edu.cn

Abstract: Achilles tendon (AT) injuries are prevalent among runners, especially in experienced runners. This study investigated how runner level and shoe longitudinal bending stiffness (LBS) interact to influence AT loading and lower-limb biomechanics. Thirty-one male rearfoot strikers (18 experienced, 13 novice) ran at 4.17 m/s in carbon-fiber shoes of three LBS levels (T1: 10.9; T2: 17.5; T3: 33.0 Nm/rad). AT force was estimated *in silico* from a subject-specific musculoskeletal model with static optimization, computed as the sum of soleus and gastrocnemius muscle forces. Discrete outcomes were analysed using mixed two-way ANOVA, and waveforms using one-dimensional Statistical Parametric Mapping (SPM1D). Experienced runners produced greater peak AT force than novice runners (p=0.038, η_p^2=0.141). LBS independently elevated peak AT force (p=0.004, η_p^2=0.182) and AT impulse (p=0.006, η_p^2=0.189), driven by an LBS-related increase in peak ankle dorsiflexion (p<0.001, η_p^2=0.493) that redirected sagittal excursion proximally. Significant runner level × LBS interactions for peak knee extension moment, peak hip external-rotation angle, and transverse-plane hip ROM showed that novice runners adapted to stiffer shoes with proximal compensations, whereas experienced runners did not. Runner level and LBS independently elevate AT loading through complementary biomechanical pathways, and novice runners rely on proximal compensations to accommodate stiffer footwear. These findings support an individualized, U-shaped view of optimal LBS.

Keywords: Achilles tendon force; longitudinal bending stiffness; musculoskeletal modeling; running biomechanics; experienced runner

1. Introduction

The Achilles tendon (AT), the strongest and thickest tendon in the human body, serves as a critical mechanical link between the calcaneus and the triceps surae muscle complex [1,2]. During locomotion, it transmits contractile forces from the calf muscles and stores and returns elastic energy during stance, thereby contributing to running economy [3–5]. However, AT's unique anatomical structure and relatively limited vascularity may impair tissue recovery after injury [6,7]. Despite its substantial load-bearing capacity, the AT is frequently injured in runners [8]. Achilles tendinopathy is one of the most prevalent overuse injuries in this population, with an incidence of 10%–20%[9]. Male runners appear to be at greater risk, and the lifetime risk in habitual runners may be as high as 52% [10]. Accordingly, understanding the mechanisms that influence AT loading and injury risk remains a priority both clinical and biomechanical research [9].

Overuse is widely regarded as a primary cause of AT injury. Running is a cyclic task that expose the AT to repetitive tensile loads that may exceed eight times body weight during each stance phase [11]. In long-distance running, the cumulative number of loading cycles is substantial. Repetitive non-uniform loading across tendon fascicles may contribute to tissue degradation [12] through heterogeneous stress distributions, inducing localized microdamage and a development of mechanically vulnerable regions within the tendon[13]. When repetitive loading continues before sufficient recovery, this damage may accumulate and eventually progress to pathological tendinopathy [14].

AT loading is closely related to lower-limb biomechanics, which may differ according to running level [15]. Previous studies have demonstrated that experienced runners typically exhibit smaller knee flexion angles, reduced ankle dorsiflexion, and lower ankle plantarflexion moments during stance phase compared to novice runners [13]. Footwear may also alter lower-limb dynamics [16]. Specifically, the longitudinal bending stiffness (LBS) of carbon-fiber plate shoes has been proposed to modify the leverage of the foot-ankle complex via a so-called teeter-totter mechanism [17]. However, recent findings suggest that increase in LBS does not necessarily produce a linear increase in ankle moment [18,19]. Instead, runners may adopt individualized neuromuscular strategies based on their physical capacity, such as increasing ankle moment directly or prolonging the push-off duration while reducing peak moment to optimize energy output [20].

Given these individualized responses to footwear stiffness, it remains unclear how runner level and shoe LBS interact to influence lower-limb biomechanics and AT loading. Because direct in-vivo measurement of AT force is invasive and technically difficult, the AT force is typically estimated via modeling methods. Conventional approaches estimate AT force by dividing the net sagittal-plane ankle moment by an estimated AT moment arm [20–22]. However, this method oversimplifies the functional anatomy of the ankle joint by assuming the Achilles tendon is the sole contributor to the net plantarflexion moment, thereby neglecting the synergistic contributions of the flexor hallucis longus, flexor digitorum longus, peroneus brevis, peroneus longus, and tibialis posterior [23–25]. These traditional methods also fail to account for the co-contraction of antagonist muscles opposing the triceps surae, which can result in inaccurate Achilles tendon load estimation [26].

Musculoskeletal modeling and simulation provide a non-invasive and cost-effective approach for estimating tendon loading during running [5,26,27]. By integrating subject-specific anatomical and biomechanical data within a musculoskeletal modeling frameworks [28,29], lower limb muscle forces during running can be estimated. The AT forces can then be derived by summing the predicted forces of the triceps surae muscles, the soleus, medial gastrocnemius, and lateral gastrocnemius, whose tendons converge to form the AT, providing a practical in silico method for quantifying tendon loading without invasive instrumentation.

Therefore, the objective of this study was to use musculoskeletal modeling to investigate the effects of runner level and shoe LBS on lower-limb biomechanics and AT loading during running. These findings may advance understanding of AT loading mechanisms and inform individualized footwear prescription and injury-prevention strategies.

2. Methods

2.1 Participants

A total of 31 healthy male runners, aged 18-50 years, were recruited for this study. All participants were right-leg dominant, exhibited a consistent rearfoot strike (RFS) pattern, and wore a standard shoe size of EUR 42. Participants were categorized into two groups based on their training experience: 13 healthy recreational runners (novice group: height 174.6 ± 3.3 cm, body mass 73.9 ± 8.7 kg) and 18 experienced runners (experienced group: height 170.8 ± 3.2 cm, body mass 62.9 ± 4.1 kg). Inclusion criteria were: (1) no history of lower-limb musculoskeletal diseases or surgery, and no significant injuries within six months prior to data collection; (2) for recreational runners, a weekly running volume of less than 10 km; and (3) for experienced runners, a minimum of three training sessions per week and a monthly running volume exceeding 100 km. Exclusion criteria were: (1) presence of any acute, infectious, or contagious diseases, or internal organ dysfunction; 2) neurological or musculoskeletal disorders with potential to cause gait abnormalities or functional impairment; (3) significant structural abnormalities, including genu valgum, genu varum, or foot arch abnormality. This study protocol received approval from the Ethics Committee of Ningbo University (TY2024028). Informed consent for publication was obtained from all individual participants included in the study.

2.2 Shoes condition

Three prototype running shoes (EUR 42) with different longitudinal bending stiffness (LBS) levels were manufactured using a standardized process by the Peak Sports Science Laboratory (Xiamen, China). All shoes shared the same basic construction: a midsole of supercritical foamed aliphatic thermoplastic polyurethane (TPU), a flexible woven mesh upper, a compression-molded outsole of polyethylene (PE) foam and cast polyurethane (CPU) composite, and an Ortholite polyurethane foam insole. LBS was manipulated by embedding full-length, spoon-shaped carbon fiber plates with differing stiffness within the TPU midsole. To minimize the potential confounding effect of shoe mass, rubber counterweights were attached to the outer periphery of each shoe so that total mass was matched across conditions. LBS was quantified using a three-point bending test, resulting in three shoe conditions: low stiffness (T1, 10.9 Nm/rad), medium stiffness (T2, 17.5 Nm/rad), and high stiffness (T3, 32.96 Nm/rad).

2.3 Data collection

Prior to data collection, anthropometric measurements were obtained. Participants first completed a 5-minute treadmill warm-up (RL2000E X 600, Robby, Sweden) at 85% of their self-selected speed wearing their own footwear. Following the warm-up, 45 retro-reflective markers were placed on predefined anatomical landmarks, including the acromion processes, anterior superior iliac spines, iliac crests, sacrum, greater trochanters, medial and lateral femoral epicondyles, medial and lateral malleoli, the first, second, and fifth metatarsal heads, and the calcaneus. Three non-collinear tracking markers were also affixed to the calcaneus. Additional tracking clusters were attached to the lateral aspect of the thighs and shanks. Participants then performed a static calibration trial in an anatomical standing posture wearing the first randomly assigned experimental shoe. Subsequently, markers on the medial malleoli, medial femoral epicondyles, and first metatarsal heads were removed for dynamic trials.

Dynamic trials were conducted on an overground runway. Participants first completed familiarization trials at a self-selected pace approximating the target speed, then performed official trials at 4.17 m/s (± 5%), monitored using a timing gate system (SWIFT Syncro Speed Measurement System). A trial was deemed successful when running speed fell within the ±5% tolerance and the participant achieved a clean foot strike on the force plate without altering their natural stride. At least three successful trials were recorded per shoe condition, with a 2-minute rest interval between conditions to reduce fatigue effects. Kinematic data were collected using a three-dimensional motion capture system comprising 12 infrared high-speed cameras (Nokov Motion Capture System, Beijing, China) at a sampling rate of 200 Hz. Ground reaction force (GRF) data were recorded synchronously using a three-dimensional force plate (Kistler 9287CA, Winterthur, Switzerland) at 1000 Hz.

2.4 Data processing

Raw motion capture data were labeled in Seek software and exported as C3D files. Coordinate systems were then transformed using a custom Python script to conform to the OpenSim convention (X-axis: anterior, Y-axis: vertical, Z-axis: right). Subsequent signal processing was performed in Python 3.11. Baseline drift in GRF data was corrected prior to filtering and segmentation. Marker trajectories were filtered using a zero-lag, fourth-order Butterworth low-pass filter with a cutoff frequency of 6 Hz; GRF data were filtered at 50 Hz[30]. Data processing focused on the stance phase of the right limb, defined by a vertical GRF threshold of 20 N to identify heel strike and toe-off events.

2.5 Musculoskeletal modeling and analysis

Biomechanical analyses were performed in OpenSim 4.5 utilizing a modified full-body musculoskeletal model. The model was originally developed by Rajagopal et al (2016)[31]. and subsequently optimized by Lai et al. [32] for high-speed movements. Specifically, the passive muscle fiber properties were adjusted in this refined model to mitigate the abnormal antagonist co-activation typically observed in muscle-driven simulations of rapid running tasks. The generic model was scaled to each participant based on anthropometric data derived from the static trial and segment masses estimated from body mass.

Using the OpenSim API in Python 3.11, a batch-processing pipeline was implemented, including inverse kinematics (IK) to estimate joint angles, inverse dynamics (ID) to estimate joint moments, static optimization (SO) to estimate individual muscle forces, body kinematics analysis to compute center-of-mass (COM) trajectories[33], and joint reaction analysis to estimate joint contact forces.

AT force F_{AT} was calculated following the approach of Almonroeder et al.[26], where the estimated muscle forces of the soleus (F_{SOL}), gastrocnemius medialis (F_{MG}), and gastrocnemius lateralis (F_{LG}) were summed to represent the total AT force (Equation (1)). AT impulse was calculated by integrating AT force over the stance phase, from initial contact to toe-off (Equation (2)). All kinetic variables were normalized to body weight (BW), and AT impulse were normalized to body mass (BW·s).

$$F_{\mathrm{AT}} = F_{\mathrm{SOL}} + F_{\mathrm{MG}} + F_{\mathrm{LG}} \quad (1)$$

$$I_{\mathrm{AT}} = \int_{t_{\mathrm{Contact}}}^{t_{\mathrm{Toe\_off}}} F_{\mathrm{AT}} \cdot dt \quad (2)$$

2.6 Statistical analysis

Statistical analyses were performed in Python 3.11. The normality of all continuous variables, including kinematics at initial contact (IC), peak joint angles and moments during stance, range of motion (ROM), and AT force and impulse, was assessed using the Shapiro-Wilk test. Data are presented as mean (standard deviation, SD). A two-way mixed analysis of variance (ANOVA) was conducted to examine the main effects of runner level (between-subject factor: experienced vs. novice) and longitudinal bending stiffness (LBS, within-subject factor: low, medium, and high), and their interaction, on lower limb biomechanics. Greenhouse-Geisser corrections were applied when the assumption of sphericity was violated according to Mauchly's test. Post-hoc pairwise comparisons were conducted using the Bonferroni correction, with statistical significance set at $p < 0.05$. Effect sizes were reported as partial eta-squared (η_p^2), and classified as small ($0.01 \leq \eta_p^2 < 0.06$), medium ($0.06 \leq \eta_p^2 < 0.14$), and large($\eta_p^2 \geq 0.14$) [34].

To evaluate the continuous biomechanical changes throughout the stance phase, one-dimensional statistical parametric mapping (SPM1D) was performed using the open source spm1d package in Python 3.11. All time-series data, including joint kinematics, kinetics, and AT force, were resampled to 101 frames using linear interpolation and normalized to the entire stance phase (0%–100%). A two-way mixed ANOVA was applied within the SPM framework to examine the main effects of runner level and LBS, as well as their interaction, across the stance phase. The significance threshold for all SPM analyses was set at $p < 0.05$.

3. Results

The effects of runner level and shoe longitudinal bending stiffness (LBS) on lower-limb biomechanics and Achilles tendon (AT) loading were demonstrated in this section. Significant findings were derived from both discrete variables, including joint kinematics at initial contact (IC), peak joint angles, range of motion (ROM), peak kinetic measures (joint moments, AT force, AT impulse), and continuous waveform data analyzed via Statistical Parametric Mapping (SPM1D). Overall, runner level was the primary determinant of AT loading and of the overall lower-limb kinematics. LBS demonstrated significant main effects on hip and ankle kinematics and proximal joint kinetics, while significant interactions were observed specifically at the hip and knee joints.

3.1 Continuous waveform analysis (SPM1D)

For the main effect of runner level, novice runner exhibited a significant greater hip flexion angle from 19% to 63% of stance and a smaller hip extension angle from 63% to 100% of stance competed to the experienced runner (p < 0.001, Figure 1A). From 0% to 42% of stance, the two groups differed significantly in hip frontal-plane angle (p < 0.001, Figure 1B): experienced runners move from slight adduction toward abduction, whereas novice runners remained slightly abducted. In late stance (61% - 100%), experienced runners demonstrated significantly greater hip abduction than novice runner. From 79% to 88% of stance, experienced runners exhibited a significantly greater hip external rotation angle compared to novice runners (p=0.039, Figure 1C). At the ankle joint, experienced runners displayed a significantly smaller ankle dorsiflexion angle from 0% to 30% of stance (p = 0.002, Figure 1E).

For lower-limb kinetics (Figure 2), experienced runners showed a significant greater ankle plantarflexion moment during 26% to 27.2% and 45% to 53% of stance (p < 0.049, Figure 2E) but demonstrated a smaller dorsiflexion moment from 76% to 80% of stance (p < 0.030, Figure 2E). Experienced runners also showed a greater knee flexion moment from 26% to 28% and from 33.80% to 34.06% of stance phase (p < 0.049, Figure 2D), but demonstrated smaller extension moment during 74% to 80.8% (p=0.002). In late stance, experienced runner produced a significantly smaller hip extension moment over 24%-28%, 30.75%-32.22%, 33.11%-34.69% and 54%-64% of stance, and a smaller hip flexion moment during 73% to 81% (all p<0.044, Figure 2A). In the hip transversal panel moment, experienced runners produced a smaller hip internal rotation moment from 48% to 49% of stance (p=0.046, Figure 2C). Additionally, experienced runners produced a significantly greater AT force than novice runners over the mid-stance phase from 0% to 0.56%, 6.59% to 10.11% and 38.8% to 55.5% of stance (all p<0.049, Figure 2F).

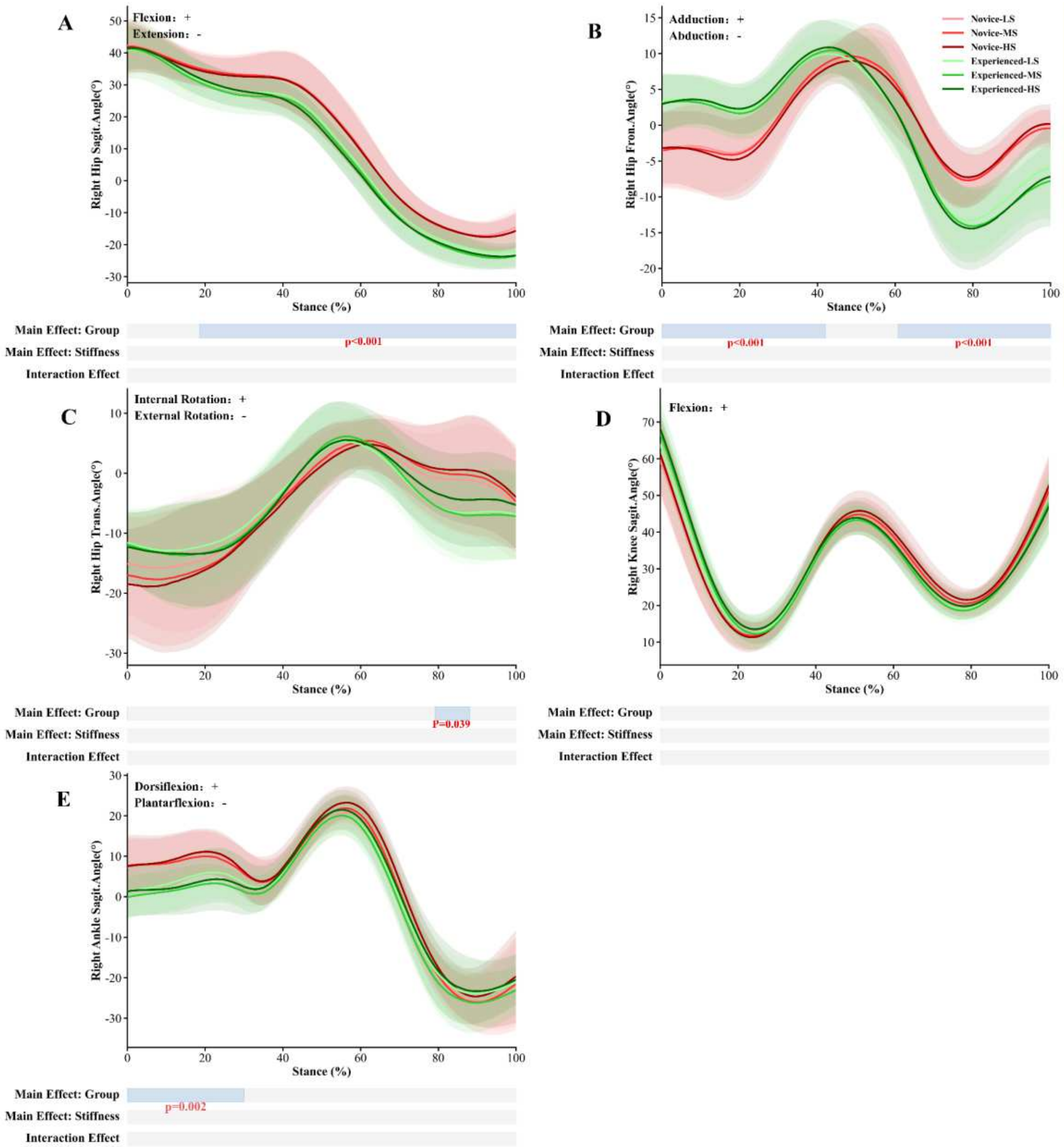

Figure 1: Statistical Parametric Mapping results for lower limb kinematics during the stance phase. (A) Right hip flexion(+)/extension(-) angle; (B) Right hip adduction(+)/ abduction(-) angle; (C) Right hip internal rotation(+)/ external rotation(-) angle; (D) Right knee flexion(+)/extension(-) angle; (E) Right dorsiflexion(+)/plantarflexion(-) angle. The solid lines represent group means, with shaded areas indicating the standard deviation. Grey horizontal bars and shaded regions denote supra-threshold clusters where significant differences between experienced and novice runners were observed (p < 0.05). The horizontal axis represents the normalized stance phase from initial contact (0%) to toe-off (100%).

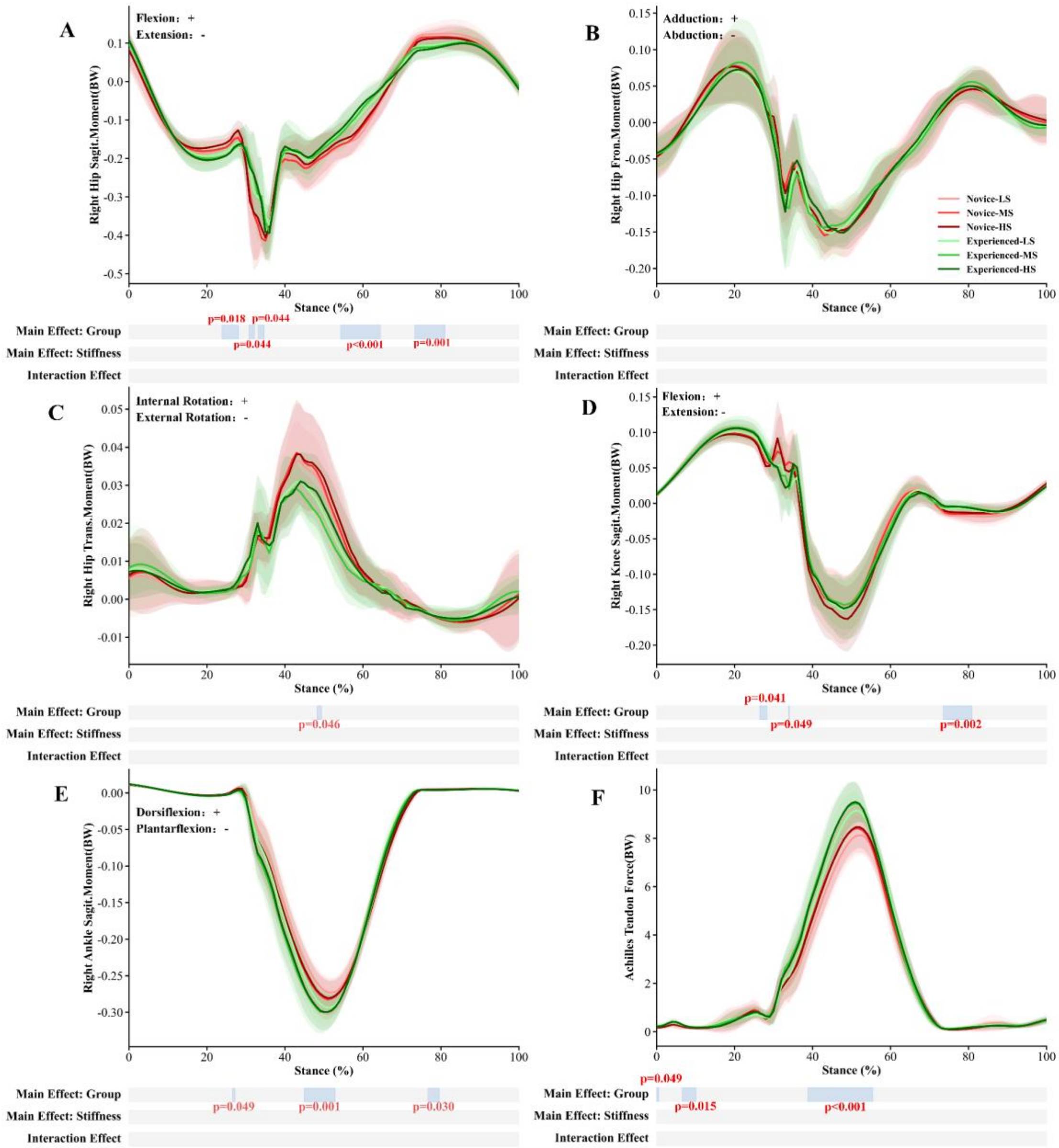

Figure 2: Statistical Parametric Mapping results for lower limb kinetics during the stance phase. (A) Right hip flexion(+)/extension(-) moment; (B) Right hip adduction(+)/abduction(-) moment; (C) Right hip internal rotation(+)/external rotation(-) moment; (D) Right knee flexion(+)/extension(-) moment; (E) Right ankle dorsiflexion(+)/plantarflexion(-) moment; (F) Right Achilles tendon force. The solid lines represent group means, with shaded areas indicating the standard deviation. Grey horizontal bars and shaded regions denote supra-threshold clusters where significant differences between experienced and novice runners were observed (p < 0.05). The horizontal axis represents the normalized stance phase from initial contact (0%) to toe-off (100%).

3.2 Key kinematics at initial contact

A significant main effect of runner level was observed for ankle dorsiflexion angle at IC ($F_{(1,29)}$=4.91, p=0.034, η_p^2=0.144, Table 1), with experienced runners exhibiting a smaller ankle dorsiflexion angle than novice runners. A significant main effect of runner level was also found for hip frontal-plane angle at IC ($F_{(1,29)}$=10.64, p=0.002, η_p^2=0.268, Table 1): experienced runners contacted the ground with the hip in slight adduction (1.64±4.04º), whereas novice runners contacted with the hip in slight abduction (-3.73±5.21º).

Table 1: Effects of runner level, shoe stiffness and their interaction on lower limb kinematic parameters

Variable	Novice Group			Experienced Group			*p-value*		
	T1	T2	T3	T1	T2	T3	G	S	G*S
$H.F/E_{IC}$	34.26 (5.14)	34.21 (5.78)	33.65 (5.37)	31.12 (5.75)	31.79 (5.89)	31.63 (5.83)	0.221	0.522	0.291
$H.Add/Abd_{IC}$	-3.35 (4.77)	-3.56 (5.57)	-4.28 (5.62)	1.53 (4.26)	1.51 (4.56)	1.88 (3.83)	**0.003**	0.859	0.143
$H.ERot_{IC}$	-13.72 (11.10)	-15.02 (10.91)	-15.41 (11.67)	-11.34 (7.57)	-11.63 (7.88)	-12.03 (9.11)	0.382	0.130	0.575
$K.F_{IC}$	11.89 (3.78)	12.98 (4.43)	11.71 (4.58)	12.31 (4.64)	13.22 (4.53)	13.54 (4.13)	0.452	0.217	0.211
$A.Dorsi/Plantar_{IC}$	10.83 (5.65)	9.82 (6.38)	11.06 (5.92)	5.20 (6.92)	5.91 (7.37)	4.52 (7.93)	**0.035**	0.818	0.060
$H.F/E_{ROM}$	61.24 (4.61)	61.99 (5.90)	60.49 (4.78)	65.68 (6.75)	67.61 (6.18)	66.51 (5.23)	**0.006**	0.290	0.276
$H.Add/Abd_{ROM}$	19.61 (5.08)	20.60 (5.15)	20.49 (5.34)	24.56 (4.48)	26.27 (6.06)	26.29 (7.09)	**0.009**	**0.034**	0.726
$H.Rot_{ROM}$	24.35 (11.42)	28.08 (12.53)	28.37 (12.01)	24.28 (6.65)	25.61 (7.73)	24.40 (7.72)	0.529	**0.003**	**0.013**
$K.F_{ROM}$	48.76 (7.38)	51.15 (5.69)	51.27 (7.42)	52.02 (9.66)	53.20 (8.53)	53.75 (6.80)	0.326	0.095	0.827
$A.Dorsi/Plantar_{ROM}$	47.61 (6.68)	49.22 (7.02)	48.79 (7.11)	44.24 (6.34)	45.37 (6.49)	45.20 (6.08)	0.129	**0.042**	0.911

T1, low stiffness; T2, medium stiffness; T3, high stiffness; IC, initial contact; ROM, range of motion; H.F/E: right hip flexion (+)/extension (-); H.Add/Abd: right hip adduction (+)/abduction (-); H.ERot: right hip internal rotation (+)/external rotation (-); K.F, right knee flexion (+)/extension (-); A.Dorsi/Plantar, right ankle dorsiflexion (+)/plantarflexion (-); H.Rot: right hip rotation; G, runner level group; S, shoes-stiffness condition; G*S, the interaction effect between runner level and shoe stiffness.

3.3 Key lower-limb joint angles and range of motion

Across the entire stance phase, a significant main effect of LBS was observed for the peak hip internal rotation angle ($F_{(2,58)}$=5.99, p=0.004, η_p^2=0.171, Table 2): peak internal rotation angle in T1 was significantly smaller than in T2 (p=0.003, Figure 3C). Peak ankle dorsiflexion also showed a significant main effect of LBS ($F_{(2,58)}$=28.30, p<0.001, η_p^2=0.493, Table 2): peak dorsiflexion angle in L1 was significantly smaller than in T2 (p<0.001) and T3 (p<0.001, Figure 3B).

A significant main effect of runner level was observed for peak hip extension angle ($F_{(1,29)}$=4.29, p=0.047, η_p^2=0.129, Table 2): experienced runners reached greater peak hip extension angle than novice runners. A significant training-level × LBS interaction effect was observed for the peak hip external rotation angle ($F_{(2,58)}$=5.57, p<0.006, η_p^2=0.161, Table 2). Follow-up simple effect analysis revealed that in the novice group, peak external rotation angle in T1 was significantly smaller than those in *T2* (*p*=0.030) and T3 (*p*=0.003, Figure 3A), whereas no significant stiffness effect in the experienced group. A significant main effect of runner level was observed for the peak hip abduction angle ($F_{(1,29)}$=5.87, *p*=0.023, η_p^2=0.168, Table 2), with experienced runners exhibited greater hip abduction angle than novice runners.

Table 2: Effects of runner level, shoe stiffness and their interaction on lower limb kinetic parameters

Variable	Novice Group			Experienced Group			*p-value*		
	T1	**T2**	**T3**	**T1**	**T2**	**T3**	**G**	**S**	**G*S**
Max H.F	42.92 (7.02)	42.71 (8.06)	42.38 (7.40)	43.35 (8.03)	44.63 (8.32)	43.89 (7.84)	0.647	0.425	0.380
Max H.Add	10.24 (2.78)	10.72 (3.58)	10.31 (3.82)	11.23 (3.28)	11.69 (4.29)	12.18 (3.48)	0.315	0.198	0.329
Max H.IRot	6.43 (5.74)	7.98 (6.44)	7.67 (6.36)	7.65 (7.34)	9.30 (7.71)	8.26 (8.19)	0.685	**0.004**	0.709
Max K.F	60.18 (8.90)	62.43 (8.08)	62.39 (9.88)	63.60 (10.69)	65.64 (9.15)	66.67 (7.02)	0.235	0.053	0.887
Max A.Dorsi	20.70 (4.38)	21.91 (3.65)	23.26 (4.21)	19.06 (4.93)	20.42 (5.06)	20.57 (4.81)	0.248	**＜0.001**	0.062
Max H.E	-18.32 (5.09)	-18.29 (5.28)	-18.11 (4.86)	-22.34 (6.66)	-22.98 (5.96)	-22.62 (6.84)	**0.047**	0.572	0.632
Max H.Abd	-9.37 (4.24)	-9.88 (4.76)	-10.18 (4.56)	-13.33 (4.52)	-14.53 (5.18)	-14.11 (6.10)	**0.022**	0.151	0.719
Max H.ERot	-17.92 (10.12)	-20.10 (9.88)	-20.69 (10.61)	-16.64 (5.99)	-16.31 (6.52)	-16.13 (6.99)	0.284	0.192	**0.006**
Max A.Plantar	-26.91 (7.36)	-27.30 (7.59)	-25.54 (7.65)	-25.17 (7.81)	-24.96 (8.20)	-24.62 (7.22)	0.547	0.100	0.345

T1, low stiffness; T2, medium stiffness; T3, high stiffness; Max, maximum; H.F/E, right hip flexion(+)/ extension(-); H.Add/Abd, right hip adduction(+)/ abduction(-); H.IRot/ERot, right hip internal(+)/ external(-) Rotation; K.F, Knee flexion is positive, with 0° at the anatomical position; R Ankle.F/E, right ankle dorsiflexion (+)/extension(-); G, runner level group; S, shoes-stiffness condition; G*S, the interaction effect between runner level and shoe stiffness.

For lower-limb joint range of motion, runner level had a significant main effect on sagittal-plane hip ROM ($F_{(1,29)}$=8.80*, p*=0.006*,* η_p^2=0.233*,* Table 1). Significant main effects of both runner level ($F_{(1,29)}$=7.75, *p*=0.009, η_p^2=0.211, Table 1) and LBS ($F_{(2,58)}$=4.20, *p*=0.020, η_p^2=0.127, Table 1) were observed for frontal-plane hip ROM: experienced runners had a significantly greater frontal-plane hip ROM, and frontal-plane ROM in T1 was significantly smaller than T2 (*p*=0.017*,* Figure 3E). Transverse-plane hip ROM showed a significant interaction effect ($F_{(2,58)}$=4.66*,* $p<0.013$*,* η_p^2=0.138*,* Table 1): in novice group, transverse-plane hip ROM in L1 was significantly smaller than T2 (*p*=0.003) and T3 (*p*=0.016*,* Figure 3D), whereas there is no significant LBS effect in the experienced group. Sagittal-plane ankle ROM showed a significant main effect of LBS ($F_{(2,58)}$=3.43*, p*=0.042*,* η_p^2=0.106*,* Table 1), with T1 ROM significantly smaller than T2 ROM (p=0.011, Figure 3F).

3.4 Joint moments

A significant training-level × LBS interaction was observed for peak knee extension moment ($F_{(2,58)}$=6.28, p=0.003, η_p^2=0.178, Table 3): in the novice group, peak knee extension moment in T3 was significantly greater than in T1 (p=0.039) and T2 (p=0.034, Figure 3H), whereas no significant stiffness effect was observed in the experienced group (Figure 3G). Significant main effect of LBS was found for peak hip adduction moment ($F_{(2,58)}$=4.47, p=0.019, η_p^2=0.134, Table 3), peak hip extension moment ($F_{(2,58)}$=6.51, p=0.004, η_p^2=0.183, Table 3) and peak knee flexion moment ($F_{(2,58)}$=4.64, p=0.022, η_p^2=0.138, Table 3). T1 produced a smaller hip adduction moment (p=0.029, Figure 3I) and a smaller extension moment (p=0.011, Figure 3J) than T2, and a smaller hip extension moment than T3 (p=0.021, Figure 3J).

3.5 AT force and impulse

Significant main effect of runner level ($F_{(1,29)}$=4.74, p=0.038, η_p^2=0.141, Table 3) and LBS ($F_{(2,58)}$=6.46, p=0.004, η_p^2=0.182, Table 3) were observed for the estimated peak AT force: experienced runners showed a significantly greater AT force than novice runners, and post-hoc analysis revealed that the T1 produced a smaller peak AT force than T3 (p=0.013, Figure 3K). A significant main effect of LBS was also observed for the AT impulse over the stance phase ($F_{(2,58)}$=6.77, p=0.006, η_p^2=0.189, Table 3), with T1 producing a smaller AT impulse than T3 (p=0.022, Figure 3L).

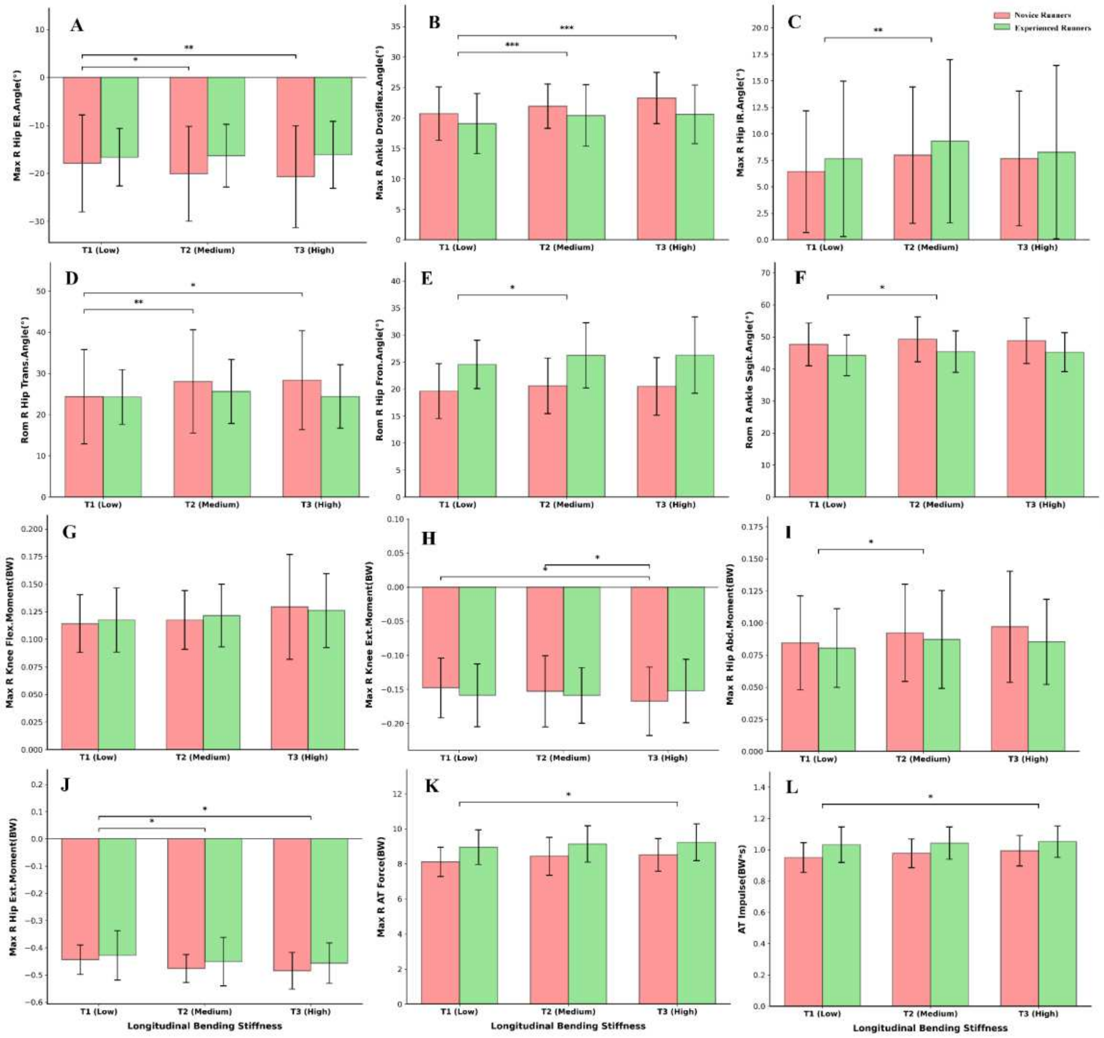

Figure 3: Post-hoc comparisons of lower limb kinematic and kinetic parameters during the stance phase. (A) Max hip external rotation angle; (B) Max ankle dorsiflexion angle; (C) Max hip internal rotation; (D) Range of motion in hip transverse plane; (E) Range of motion in hip frontal plane; (F) Range of motion in ankle sagittal plane; (G) Max knee flexion moment; (H) Max knee extension moment; (I) Max hip abduction moment; (J) Max hip extension moment; (K) Max Achilles tendon (AT) force; (L) Achilles tendon impulse. T1, T2, and T3 represent low, medium, and high longitudinal bending stiffness (LBS), respectively. Bars represent mean values, and error bars indicate one standard deviation. Asterisks and horizontal lines denote statistically significant differences between groups or conditions (**p*< 0.05, ***p*< 0.01, ****p*< 0.001).

Table 3: Effects of runner level, shoe stiffness on Achilles tendon loading and lower limb kinetic parameters

Variable	Novice Group			Experienced Group			*p-value*		
	T1	**T2**	**T3**	**T1**	**T2**	**T3**	**G**	**S**	**G*S**
AT Impulse (BW·S)	0.95 (0.09)	0.98 (0.09)	0.99 (0.10)	1.03 (0.11)	1.04 (0.10)	1.05 (0.10)	0.065	**0.007**	0.321
Max H.FM (BW)	0.135 (0.03)	0.124 (0.03)	0.124 (0.02)	0.117 (0.03)	0.118 (0.02)	0.117 (0.02)	0.227	0.339	0.175
Max H.AddM (BW)	0.085 (0.037)	0.092 (0.038)	0.097 (0.043)	0.080 (0.031)	0.087 (0.038)	0.085 (0.033)	0.588	**0.019**	0.381
Max H.IRotM (BW)	0.039 (0.010)	0.040 (0.013)	0.042 (0.013)	0.038 (0.012)	0.040 (0.013)	0.038 (0.010)	0.716	0.310	0.266
Max K.FM (BW)	0.114 (0.026)	0.117 (0.027)	0.129 (0.048)	0.118 (0.029)	0.122 (0.028)	0.126 (0.033)	0.900	**0.023**	0.579
Max A.DorsiM (BW)	0.012 (0.002)	0.012 (0.001)	0.012 (0.001)	0.012 (0.002)	0.012 (0.002)	0.012 (0.001)	0.768	0.262	0.720
Max H.EM(BW)	-0.444 (0.054)	-0.476 (0.051)	-0.484 (0.067)	-0.428 (0.090)	-0.451 (0.089)	-0.456 (0.074)	0.359	**0.004**	0.812
Max H.AbdM(BW)	-0.170 (0.03)	-0.178 (0.03)	-0.179 (0.02)	-0.192 (0.03)	-0.192 (0.02)	-0.186 (0.02)	0.348	0.790	0.486
Max H.ERotM(BW)	-0.010 (0.005)	-0.010 (0.004)	-0.010 (0.005)	-0.008 (0.005)	-0.008 (0.003)	-0.008 (0.004)	0.115	0.736	0.844
Max K.EM(BW)	-0.148 (0.044)	-0.153 (0.052)	-0.167 (0.050)	-0.159 (0.046)	-0.159 (0.041)	-0.152 (0.047)	0.972	0.538	**0.003**
Max A. PlantarM(BW)	-0.274 (0.022)	-0.283 (0.029)	-0.283 (0.024)	-0.291 (0.025)	-0.294 (0.028)	-0.296 (0.026)	0.122	0.104	0.552
Max AT Force (BW)	8.11 (0.84)	8.43 (1.08)	8.51 (0.93)	8.95 (0.99)	9.13 (1.04)	9.23 (1.05)	**0.038**	**0.004**	0.756

T1, Low Stiffness; T2, Medium Stiffness; T3, High Stiffness; Max, Characteristic Peak; H.FM/EM, Right Hip Flexion Moment(+)/Extension Moment(-); H.AddM/AbdM, Right Hip Adduction Moment(+)/Abduction Moment(-); H.IRotM/ERotM, Right Hip Internal (+)/External(-) Rotation Moment; K.F/EM, Right Knee Flexion Moment(+)/Extension Moment(-); A.DorsiM/PlantarM, Right Ankle Dorsiflexion Moment(+)/Plantarflexion Moment(-); AT Force, Achilles Tendon Force; AT Impulse, Achilles Tendon Impulse; G, Runner Level Group; S, Shoes-stiffness condition; G*S, Interaction Effect Between Runner Level And Shoe Stiffness.

4. Discussion

This study examined the interaction effects of shoe longitudinal bending stiffness (LBS) and runner level on lower-limb biomechanical characteristics and Achilles tendon (AT) loading during overground running in healthy male rearfoot strikers. AT force was estimated *in silico* using a full-body musculoskeletal model with static optimization, and derived as the sum of the soleus, medial gastrocnemius, and lateral gastrocnemius muscle forces. Three main findings emerged: (1) experienced runners exhibited significantly greater peak estimated AT force than novice runners and adopted distinct lower-limb biomechanical strategies across the stance phase; (2) LBS induced significant effects on hip joint kinematics and kinetics and on AT loading; (3) significant runner level × LBS interaction for the peak hip extension moment, transverse-plane hip ROM and peak knee extension moment indicated that experienced and novice runners responded differently to stiffness manipulation at proximal joints.

Compared with novice runners, experienced runners exhibited significantly greater estimated peak AT force, and this group difference was corroborated by both the discrete feature analysis and continuous SPM1D mapping (Figure 2F), which localized the between-group difference to early stance (6.59%-10.11%) and propulsion (38.8%-55.5%). This is consistent with Yan et al.[30], who reported higher ankle plantarflexion moments in more experienced runners, suggesting that long-term training improves triceps surae function and raises baseline AT loading.

AT impulse showed the same direction (experience > novice), but only reached marginal significance (p=0.064, η_p^2=0.113). The moderate effect size combined with the borderline p-value suggests the trend is likely real but constrained by the present sample size. This finding contradict Li et al.[13], who reported greater AT impulses in novice runners. This discrepancy is likely attributable to running speeds. Li et al. tested at 3.33 m/s, whereas we tested at 4.17 m/s. At slower speeds, the longer contact time observed in novice runners can drive higher per-step impulse despite lower per-step peak force, whereas at faster paces the propulsive demand on the triceps surae dominates and the experienced runners kinetic advantage becomes apparent.

The kinematic and kinetic patterns observed in experienced runners offer a comprehensive mechanical explanation for their higher AT loading. At initial contact, experienced runners landed with a smaller ankle dorsiflexion angle (a flatter foot-strike geometry) and with the hip in slight adduction, in contrast to the slight abduction observed in novice runners. Across the stance phase, SPM1D analysis showed that experienced runners maintained a more extended hip from 19% of stance through toe-off and adopted a more abducted hip in late stance. The corresponding kinetic SPM analysis (Figure 2) revealed a distally-loaded mid-stance pattern: experienced runners produced significantly greater ankle plantarflexion moments during propulsion (26%–27% and 45%–53%) while generating smaller hip extension moments through much of mid-stance.

This distal-dominated strategy directs more mechanical demand toward the triceps surae, which contributes approximately 41% of total positive lower-limb work during running [15,35]. By transitioning rapidly from a flatter foot strike into push-off and engaging the medial gastrocnemius more effectively via a hip transition from adduction to abduction with external rotation, experienced runners optimize propulsive force production at the cost of greater per-stride AT tensile load [30]. Although these adaptations enhance propulsion, it simultaneously impose higher chronic tensile stress on the tendon. According to the *non-uniform loading theory* [27], the confluence of high-intensity, repetitive loading cycles induces maladaptive stress distribution across tendon fascicles, initiating damage accumulation at the fibrillar scale and eventually producing localized “weak zones” within the macro-structure[36]. Combined with the greater training volume characteristic of experienced runners, this per-step loading profile provides a biomechanical rationale for the ~52% lifetime AT injury risk reported in this population[37,38].

LBS contributed a substantial mechanical effect on top of these baseline group differences [13]. The largest single effect in our dataset was an LBS-driven increase in peak ankle dorsiflexion (η^2_p = 0.493), accompanied by an increase in sagittal-plane ankle ROM. Because carbon-fiber plates stiffen the metatarsophalangeal joint rather than the talocrural joint, sagittal excursion that would normally occur at the forefoot is redirected proximally to the ankle. This redirection in turn raised peak hip extension, hip adduction, and knee flexion moments, indicating a more aggressive movement strategy in stiffer shoes [39,40]. Both peak AT force and AT impulse rose with LBS, demonstrating that the mechanical chain linking forefoot stiffening to AT loading is intact and operative across runners. Notably, the LBS-driven changes in joint ROM and peak angles did not follow a strictly linear trajectory: further increases from T2 to T3 did not produce proportionally larger kinematic changes, suggesting a non-linear response. This is consistent with the *U-shaped* relationship between LBS and the lower-limb kinetic chain [41]. Each joint and biomechanical parameter likely has its own stiffness threshold; once this threshold is exceeded, the effect on the lower-limb kinetic chain may plateau or even diminish [39].

A significant interaction between shoe stiffness and runner level was observed for the peak knee extension moment, hip external rotation angle and transverse-plane hip ROM. Novice runners up-regulated knee extension moment, hip external rotation, and transverse-plane hip ROM in response to increasing LBS, whereas experienced runners remained stable. Stiffer shoes therefore appear to elevate proximal kinematic and kinetic demand in novice runners.

Whether this elevation is beneficial is open to question. Elevated knee extension moments directly intensify quadriceps work demand, which raises patellofemoral joint contact stress and subsequently increases the risk of patellofemoral pain syndrome [22]. The interaction pattern observed in this study is consistent with the *individual optimal LBS* concept: Roy et al. [41] identified a U-shaped relationship between LBS and running economy, with performance gains maximized only when footwear stiffness matches the runner's specific neuromuscular and structural capacity. The positioning of this individual optimum is further modulated by running speed and triceps surae strength [40,42]. In novice runners, whose triceps surae capacity and inter-joint coordination are typically less developed, increasing LBS appears to shift the proximal joints into less stable, less efficient configurations rather than augmenting performance.

Our findings identify two distinct injury-risk profiles. Experienced runners carry an elevated baseline AT loading driven by a propulsion optimised distal kinetic strategy; further increases in LBS amplify this load and, combined with high training volume, plausibly contribute to the high lifetime AT injury risk reported in this population [9]. Novice runners, in contrast, do not carry the same baseline AT load, but adopt unstable proximal compensations, with greater knee extension moments, larger transverse-plane hip motion, and larger peak hip external-rotation angles in stiffer shoes, exposing them to acute risk at the knee and hip rather than at the tendon. Importantly, Hannigan et al. [43] indicate that this additional proximal torque burden may also offset the energetic benefits that carbon-fibre plates ordinarily provide at the ankle, so the trade-off is not simply one of risk against performance gain.

These findings argue against a simple "stiffer is better" approach to carbon-fibre footwear prescription. Instead, LBS should be matched to the runner's training level: experienced runners may benefit from moderate stiffness that supports propulsion without disproportionately elevating AT load, whereas novice runners may be better served by lower stiffness until their proximal control and triceps surae capacity are sufficient to absorb the redistributed kinetic demand. This recommendation provides a biomechanical basis for individualised footwear prescription, consistent with the U-shaped, individual-optimum framework [41].

This study has several limitations. First, only male runners were tested at a single speed (4.17 m/s). Because both sex and running speed influence AT loading and footwear biomechanics, the findings may not generalize to female runners or to slower training paces. Second, AT force was estimated *in silico* using a subject-specific musculoskeletal model scaled from a generic model, combined with static optimization. This approach is well validated for relative comparisons, but absolute force magnitudes carry inherent uncertainty.

5. Conclusion

Runner level was the principal determinant of Achilles tendon loading. Experienced runners used a propulsion-oriented, distally loaded mid-stance strategy that produced higher per-stride AT force. Shoe LBS added a significant effect by shifting sagittal excursion proximally and increasing both peak AT force and AT impulse. Novice and experienced runners did not respond to LBS in the same way: novice runners compensated through proximal kinetic and transverse-plane hip adjustments that experienced runners did not show. These findings support a U-shaped, individualized view of optimal LBS and argue against a one-size-fits-all “stiffer is better” approach to carbon-fiber footwear prescription.

Acknowledgements

The authors thank all study participants and the Peak Sport Science Laboratory for assistance with data collection.

Funding

This work was supported by the National Natural Science Foundation of China (31871204, 12572368); the 2025 Ningbo University High-Level Science and Technology Project Incubation Program (GJPY2025027); and the

Foundation of Key Laboratory of Orthopedics and Traumatology of Traditional Chinese Medicine and Rehabilitation, Ministry of Education, Fujian university of TCM (XGS2024004); and K.C. Wong Magna Fund in Ningbo University.

Author contributions

Ye Ma and Mianfang Ruan conceived and designed the study. Hao Yuan and Shixin Lin performed the experiments. Dongwei Liu and Hao Yuan analyzed the data. Shixin Lin and Hao Yuan wrote the main manuscript text. Jiayin Shao and Shixin Lin prepared all the figures. All authors reviewed and approved the final manuscript.

Competing interests

The authors declare no competing interests.

Data availability

Raw data will be made available on reasonable request to the corresponding author Ye Ma.

Ethics declarations

The study was conducted according to the guidelines of the Declaration of Helsinki and approved by the Ethics Committee of Faculty of Sports Sciences at Ningbo University with the registration number of TY2024028. Written informed consent was obtained from all participants.

References

[1] Alrashidi, Y., Alrabai, H. M., Alsayed, H. & Valderrabano, V. Achilles tendon in sport. *Sports Orthop.* **31**, 282–292 (2015). https://doi.org/10.1016/j.orthtr.2015.09.009.

[2] O'Brien, M. The anatomy of the Achilles tendon. *Foot and ankle clinics* **10**, 225–238 (2005). https://doi.org/10.1016/j.fcl.2005.01.011.

[3] Kubo, K., Tabata, T., Ikebukuro, T., Igarashi, K. & Tsunoda, N. A longitudinal assessment of running economy and tendon properties in long-distance runners. *J. Strength Cond. Res.* **24**, 1724–1731 (2010). https://doi.org/10.1519/JSC.0b013e3181ddf847.

[4] Benjamin, M. *et al.* Where tendons and ligaments meet bone: attachment sites ('entheses') in relation to exercise and/or mechanical load. *J. Anat.* **208**, 471–490 (2006). https://doi.org/10.1111/j.1469-7580.2006.00540.x.

[5] Rice, C. M. Modelling of the achilles and patella tendon forces during treadmill running. (Stellenbosch: Stellenbosch University, 2021). http://hdl.handle.net/10019.1/110106.

[6] Doral, M. N. *et al.* Functional anatomy of the Achilles tendon. *Knee Surgery, Sports Traumatology, Arthroscopy* **18**, 638–643 (2010). https://doi.org/10.1007/s00167-010-1083-7.

[7] Ulreich, N., Kainberger, F., Huber, W. & Nehrer, S. Die achillessehne im sport. *Radiologe* **42**, 811–817 (2002). https://doi.org/10.1007/s00117-002-0800-8.

[8] Lyght, M., Nockerts, M., Kernozek, T. W. & Ragan, R. Effects of foot strike and step frequency on Achilles tendon stress during running. *Journal of applied biomechanics* **32**, 365–372 (2016). https://doi.org/10.1123/jab.2015-0183.
[9] Munteanu, S. E. & Barton, C. J. Lower limb biomechanics during running in individuals with achilles tendinopathy: a systematic review. *Journal of foot and ankle research* **4**, 15 (2011). https://doi.org/10.1186/1757-1146-4-15.
[10] De Vos, R. J. *et al.* Platelet-rich plasma injection for chronic achilles tendinopathy: a randomized controlled trial. *JAMA* **303**, 144–149 (2010). https://doi.org/10.1001/jama.2009.1986.
[11] Van Hooren, B., van Rengs, L. & Meijer, K. Per-step and cumulative load at three common running injury locations: the effect of speed, surface gradient, and cadence. *Scand. J. Med. Sci. Sports.* **34**, e14570 (2024). https://doi.org/10.1111/sms.14570.
[12] Khan, K. M., Cook, J. L., Kannus, P., Maffulli, N. & Bonar, S. F. Time to abandon the "tendinitis" myth: painful, overuse tendon conditions have a non-inflammatory pathology. in *Bmj* vol. 324 626–627 (British Medical Journal Publishing Group, 2002). https://doi.org/10.1136/bmj.324.7338.626.
[13] Li, Y., Nie, Y., Zhang, X. & Gu, Y. Effects of footwear and foot strike patterns on patellofemoral joint and Achilles tendon loading in novice runners and experienced runners. *Frontiers in Sports and Active Living.* **7**, 1610514 (2025). https://doi.org/10.3389/fspor.2025.1610514.
[14] Al Makhzoomi, A. K., Kirk, T. B. & Allison, G. T. A multiscale study of morphological changes in tendons following repeated cyclic loading. *J. Biomech.* **128**, 110790 (2021). https://doi.org/10.1016/j.jbiomech.2021.110790.
[15] Novacheck, T. F. The biomechanics of running. *Gait & posture.* **7**, 77–95 (1998). https://doi.org/10.1016/S0966-6362(97)00038-6.
[16] Sun, X., Lam, W.-K., Zhang, X., Wang, J. & Fu, W. Systematic review of the role of footwear constructions in running biomechanics: Implications for running-related injury and performance. *Journal of sports science & medicine.* **19**, 20 (2020). https://doi.org/PMC7039038.
[17] Nigg, B. M., Cigoja, S. & Nigg, S. R. Teeter-totter effect: a new mechanism to understand shoe-related improvements in long-distance running. *British Journal of Sports Medicine.* **55**, 462–463 (2021). https://doi.org/10.1136/bjsports-2020-102550.
[18] Healey, L. A. & Hoogkamer, W. Longitudinal bending stiffness does not affect running economy in nike vaporfly shoes. *J. Sport Health Sci.* **11**, 285–292 (2022). https://doi.org/10.1016/j.jshs.2021.07.002.
[19] Van Kouwenhove, L., Verkerke, G. J., Postema, K., Dekker, R. & Hijmans, J. M. Effects of Longitudinal Bending Stiffness of forefoot rocker profile shoes on ankle kinematics and kinetics. *Gait & Posture.* **90**, 326–333 (2021). https://doi.org/10.1016/j.gaitpost.2021.09.188.
[20] Chen, H. *et al.* Effects of footwear with different longitudinal bending stiffness on biomechanical characteristics and muscular mechanics of lower limbs in adolescent runners. *Frontiers in physiology.* **13**, 907016 (2022). https://doi.org/10.3389/fphys.2022.907016.
[21] Lee, K. K., Ling, S. K. & Yung, P. S. Controlled trial to compare the Achilles tendon load during running in flatfeet participants using a customized arch support orthoses vs an orthotic heel lift. *BMC musculoskeletal disorders.* **20**, 535 (2019). https://doi.org/10.1186/s12891-019-2898-0.
[22] Zhang, X., Fu, B., Li, Y., Deng, L. & Fu, W. Effects of habitual foot strike patterns on patellofemoral joint and Achilles tendon loading in recreational runner. *Gait &*

Posture. **117**, 121–128 (2025). https://doi.org/10.1016/j.gaitpost.2024.12.017.
[23] Holzer, D., Paternoster, F. K., Hahn, D., Siebert, T. & Seiberl, W. Considerations on the human achilles tendon moment arm for in vivo triceps surae muscle–tendon unit force estimates. *Sci. Rep.* **10**, 19559 (2020). https://doi.org/10.1038/s41598-020-76625-x.
[24] Masood, T. *et al.* Differential contributions of ankle plantarflexors during submaximal isometric muscle action: A PET and EMG study. *J. Electromyogr. Kinesiol.* **24**, 367–374 (2014). https://doi.org/10.1016/j.jelekin.2014.03.002.
[25] Brockett, C. L. & Chapman, G. J. Biomechanics of the ankle. *Orthop. trauma.* **30**, 232–238 (2016). https://doi.org/10.1016/j.mporth.2016.04.015.
[26] Almonroeder, T., Willson, J. D. & Kernozek, T. W. The effect of foot strike pattern on Achilles tendon load during running. *Annals of biomedical engineering.* **41**, 1758–1766 (2013). https://doi.org/10.1007/s10439-013-0819-1.
[27] Mylle, I., Funaro, A., Crouzier, M., Bogaerts, S. & Vanwanseele, B. Achilles tendon compliance influences tendon loading more than Achilles tendon twist in Achilles tendinopathy: a musculoskeletal modeling approach. *Frontiers in Bioengineering and Biotechnology.* **12**, 1399611 (2024). https://doi.org/10.3389/fbioe.2024.1399611.
[28] Koller, W., Baca, A. & Kainz, H. Impact of scaling errors of the thigh and shank segments on musculoskeletal simulation results. *Gait Posture.* **87**, 65–74 (2021). https://doi.org/10.1016/j.gaitpost.2021.02.016.
[29] Delp, S. L. *et al.* OpenSim: open-source software to create and analyze dynamic simulations of movement. *IEEE Trans. Bio-Med. Eng.* **54**, 1940–1950 (2007). https://doi.org/10.1109/TBME.2007.901024.
[30] Yang, H., Cai, Y., Li, K., Wang, X. & Liu, T. Effects of varying longitudinal bending stiffness in running shoes on lower limb biomechanics of elite marathon runners. *Frontiers in Sports and Active Living.* **7**, 1608092 (2025). https://doi.org/10.3389/fspor.2025.1608092.
[31] Rajagopal, A. *et al.* Full-body musculoskeletal model for muscle-driven simulation of human gait. *IEEE Trans. Bio-Med. Eng.* **63**, 2068–2079 (2016). https://doi.org/10.1109/TBME.2016.2586891.
[32] Lai, A. K., Arnold, A. S. & Wakeling, J. M. Why are antagonist muscles co-activated in my simulation? A musculoskeletal model for analysing human locomotor tasks. *Ann. Biomed. Eng.* **45**, 2762–2774 (2017). https://doi.org/10.1007/s10439-017-1920-7.
[33] Bedo, B. L. *et al.* BOPS: a matlab toolbox to batch musculoskeletal data processing for OpenSim. *Comput. Methods Biomech. Biomed. Eng.* **24**, 1104–1114 (2021). https://doi.org/10.1080/10255842.2020.1867978.
[34] Cohen, J. Eta-squared and partial eta-squared in fixed factor ANOVA designs. *Educ. psychol. meas.* **33**, 107–112 (1973). https://doi.org/10.1177/001316447303300111.
[35] Kulmala, J.-P. *et al.* Walking and running require greater effort from the ankle than the knee extensor muscles. *Med. Sci. Sports Exercise.* **48**, 2181–2189 (2016). https://doi.org/10.1249/MSS.0000000000001020.
[36] Lorimer, A. V. & Hume, P. A. Stiffness as a risk factor for Achilles tendon injury in running athletes. *Sports Medicine.* **46**, 1921–1938 (2016). https://doi.org/10.1007/s40279-016-0526-9.
[37] Yu, C., Deng, L., Li, L., Zhang, X. & Fu, W. Exercise effects on the biomechanical properties of the Achilles tendon—a narrative review. *Biology.* **11**, 172 (2022). https://doi.org/10.3390/biology11020172.

[38] Kujala, U. M., Sarna, S. & Kaprio, J. Cumulative incidence of achilles tendon rupture and tendinopathy in male former elite athletes. *Clinical Journal of Sport Medicine.* **15**, 133–135 (2005). https://doi.org/10.1097/01.jsm.0000165347.55638.23.
[39] Oh, K. & Park, S. The bending stiffness of shoes is beneficial to running energetics if it does not disturb the natural MTP joint flexion. *Journal of biomechanics.* **53**, 127–135 (2017). https://doi.org/10.1016/j.jbiomech.2017.01.014.
[40] Willwacher, S., König, M., Braunstein, B., Goldmann, J.-P. & Brüggemann, G.-P. The gearing function of running shoe longitudinal bending stiffness. *Gait & posture.* **40**, 386–390 (2014). https://doi.org/10.1016/j.gaitpost.2014.05.005.
[41] Roy, J.-P. R. & Stefanyshyn, D. J. Shoe midsole longitudinal bending stiffness and running economy, joint energy, and EMG. *Medicine and science in sports and exercise.* **38**, 562–569 (2006). https://doi.org/10.1249/01.mss.0000193562.22001.e8.
[42] Day, E. & Hahn, M. Optimal footwear longitudinal bending stiffness to improve running economy is speed dependent. *Footwear Science.* **12**, 3–13 (2020). https://doi.org/10.1080/19424280.2019.1696897.
[43] Hannigan, J. J., Westley, L. & Jin, L. Injury and performance-related running biomechanics in advanced footwear technology compared to minimalist footwear. *Footwear Science.* **16**, 115–121 (2024). https://doi.org/10.1080/19424280.2024.2327317.

Supplementary Files

This is a list of supplementary files associated with this preprint. Click to download.

- supplementFigureV02.pdf